

# *Ab initio* calculations of quasiparticle band structure in correlated systems: LDA++ approach

A.I. Lichtenstein<sup>1</sup> and M.I. Katsnelson<sup>2</sup>

<sup>1</sup>*Forschungszentrum Jülich, Germany*

<sup>2</sup>*Institute of Metal Physics,  
Ekaterinburg 620219, Russia*

We discuss a general approach to a realistic theory of the electronic structure in materials containing correlated d- or f- electrons. The main feature of this approach is the taking into account the energy dependence of the electron self-energy with the momentum dependence being neglected (local approximation). It allows us to consider such correlation effects as the “non-Fermi-step” form of the distribution function, the enhancement of the effective mass including “Kondo resonances”, the appearance of the satellites in the electron spectra etc. To specify the form of the self-energy, it is useful to distinguish (according to the ratio of the on-site Coulomb energy  $U$  to the bandwidth  $W$ ) three regimes - strong, moderate and weak correlations. In the case of strong interactions ( $U/W > 1$  - “rare-earth system”) the Hubbard-I approach is the most suitable. Starting from an exact atomic Green function with the constrained density matrix  $n_{mm'}$  the band structure problem is formulated as the functional problem on  $n_{mm'}$  for f-electrons and the standard LDA-functional for delocalized electrons. In the case of moderate correlations ( $U/W \sim 1$  - “metal -insulator regime, Kondo systems”) we start from the  $d = \infty$  dynamical mean field iterative perturbation scheme (IPS) of G. Kotliar et. al. and also make use of our multiband atomic Green function for constrained  $n_{mm'}$ . Finally for the weak interactions ( $U/W < 1$  - “transition metals”) the self-consistent diagrammatic fluctuation-exchange (FLEX)-approach of N. Bickers and D. Scalapino is generalized to the realistic multiband case. We presents two-band, two-dimensional model calculations for all three regimes. A realistic calculation in Hubbard-I scheme with the exact solution of the on-site multielectron problem for f(d)- shells was performed for mixed-valence 4f compound TmSe, and for the classical Mott insulator NiO.

71.10.+x,74.20.Mn,74.72.Bk

## I. INTRODUCTION

A general accurate description of the electronic structure of materials with correlated electrons has yet to be developed. Such materials include the high- $T_c$  and colossal magnetoresistance (CMR) materials, as well as the mixed-valence and heavy-fermion compounds. All these systems demonstrate essentially many-particle (correlation) features in their excitation spectrum and ground-state properties, the usual language of one-electron band theory being inadequate to describe such features even qualitatively: e.g., the problem of Mott insulators, the heavy-fermion behavior in some rare-earth compounds, satellites and “mid-gap states” in electron spectra etc. (see e.g. recent reviews [1–4]). Such effects as the metal-insulator transition, Kondo effect, and others, which helps to understand the basic physics in these strongly correlated materials, is usually considered in the framework of simplified models such as the Hubbard model, Anderson model, s-f exchange model and other correlation models. Nevertheless the complexity of the crystals containing 10-15 different atoms per unit cell, interactions between electronic and lattice degrees of freedom demands a more detailed investigation of the energy bands in such systems. The only general first-principles approach that takes into account in practice specific peculiarities of the electronic structure in real compounds are those based on the density functional theory (DFT) [5]. The vast majority of practical DFT applications today are based on the local density approximation (LDA), which treats the exchange-correlation (XC) part of an effective single-particle DFT potential as a density dependent XC-potential, taken from the exact quantum Monte-Carlo (QMC) results for the homogeneous electron gas. There are many successes but also some failures of LDA approach [6], related to the simple fact that in cases where some portion of electronic structure is better described in terms of atomic-like electronic states, the homogeneous electron gas approximation is not a good starting point. Another limitation of LDA theory is that it is only a ground state scheme and the one-particle band-structure itself has, generally speaking, no proper meaning. Recently the time-dependent (TD-LDA) approach has been applied for calculations of excitation energies [7,8], but the TD-LDA effective potential is not known as good as LDA one. On the other hand, exact QMC calculations for real materials which have tedious first-principle Hartree-Fock band structure as zero order approximations is still a challenging problem of solid state theory [9–11].

In this situation it is useful to have simple and accurate scheme that could still capture the most important properties

of real electronic structure and at the same time could take into account the most important correlation effects. One of the first successful approach in this line was the GW-approximation [12] for quasiparticle spectra in solids with the self-energy related to a “bare” Green function (G) and a screened Coulomb interaction (W). Self-consistent GW calculations basing on the LDA band structure gives much better description of a Mott insulator such as NiO than does pure LDA [13]. Still, the non-local Coulomb interactions make such type of calculations really time consuming. For the purpose of only band-structure investigations one could use a simplified time-independent GW-scheme or so-called screen-exchange (sX-LDA) approach [14,15]. The later approach has of the same drawbacks as does Hartree-Fock approximation and did not suitable for strongly correlated systems. A different way to incorporate some correlation effect in the systems with localized d- or f-states was successfully done in so-called LDA+U method [16]. In this case a simple mean-field Hubbard-like term is added to LDA functionals for the localized state and care must be taken for correction of the LDA double-counting [17]. This approach can also be viewed as a density functional theory, since the U terms that depend on occupation number for localized electrons is a functional of the total density. So one just uses the LDA-functional for delocalized electrons and improved LDA+U functional for localized atomic-like states. This approach produces a more reliable description of the electronic and crystal structure of correlated materials with charge, spin, and orbital ordering than does the LSDA scheme [18]. But LDA+U scheme, as well as the approach based on the so called self-interaction corrections (SIC) [19], has one intrinsic shortcoming related with a mean-field approximation. It is well known (see e.g. [20,21]) that the most interesting correlation effects in quasiparticle spectra such as the mass enhancement, damping, the difference of the distribution function from the “Fermi step” are connected with the energy dependence of the self-energy  $\Sigma(\omega)$ , so one needs to generalize LDA+U approach to include dynamical effects. Such scheme we would like to call “LDA++” [22]. One can mention few successful attempts in this directions: quasiparticle (QP) band structure calculation of Fe, Co and Ni [23–25] as well as heavy fermion system [26,27] using simplest second order local approximation for the self-energy; QP-band structure of NiO [28,29] using 3-body Faddeev approximation; RPA-like approach for HTSC [30] and non-crossing approximations (NCA) for Kondo systems [31]. At the same time, a criterion for the applicability of specific approximations used in these works was not clear.

In this paper we propose a general scheme for LDA++ band structure calculations for real materials with the different strength of electronic correlations. It is not very efficiently from the computational point of view (as well as not very reasonable from the purely theoretical one) to use the only LDA++ scheme for materials with a different electron-electron interactions. In accordance with the ratio of average on-site Coulomb parameter U to the relevant valence band width W, it is useful to distinguish three regimes of weak, moderate and strong correlations.

The simplest case of weak correlations ( $U/W < 1$  - “transition metals”) we could use the self-consistent diagrammatic approach. The most convenient way is the conserving fluctuation exchange (FLEX) approximation [32] and we will use the multiband generalizations for LDA++ weak correlation scheme. The characteristic feature of this renormalized band regime that no additional states appears in the electronic structure due to interactions or, more exactly, there is one-to-one correspondence of quasiparticle states with and without interaction. Roughly speaking, the shape of energy bands may be changed but there are no band splitting, or presence of additional bands. The most interesting physical phenomena in this case are the renormalization of the effective masses, flattening of Van Hove singularities etc.

In the case of very strong interactions ( $U/W > 1$  - “rare-earth system”) we will start with exact atomic Greens function for f-states and use the Hubbard-I approximation (HIA) [33] to analyze the spectrum of f-systems. This approach also may be applied to such d-systems as Mott insulators with very narrow d-bands. For this situation the electronic structure of solids will combine the many-body structure of f(d)-ions and broad bands from delocalized electrons. In this case such phenomena as multiplet structure, satellites in photoelectron spectra, the narrowing of the electron bands depending on the magnetic ordering etc are the subjects of main interests.

In the most difficult case of strongly correlated physics ( $U/W \sim 1$  - “metal-insulator transition” regime or “Kondo systems”) we will use the interpolation scheme based on dynamical mean field theory (DMFT) [3]. In this situation we will have a “three-peak structure” from a single correlated band, consisting of upper and lower Hubbard bands and Kondo resonance near the Fermi energy. Such scheme is the most accurate, but also the most time consuming, and it is difficult to make a self-consistent calculations for a large system. The other point of view of the different LDA++ schemes could be related to the different energy scales for the spectrum of correlated materials: if one is interested in the large energy scale that HIA-approximation is sufficient for spectroscopic purposes. If we like to describe low-energy scale of a system like doped Mott insulators or mixed valence systems then DMFT approach is the most adequate.

The common feature of all LDA++ methods is the matrix form of self-energy since electron-electron correlations can not be diagonalized neither in band index  $n$  nor in orbital indices  $lm$ . This peculiarity of multi-band Hubbard interactions are normally ignored and only few examples of matrix self-energy exist for transition metal with LDA second-order perturbation scheme [23,25], transition-metal oxides within 3-body Faddeev approximation [29] and for two-band Hubbard model for investigation of orbital and magnetic instabilities [34].

This paper is organized as follows. In Sec. II. we will give a general description of different correlations scheme to the dynamical mean field band structure calculations. The simple two-bands model (Sec.III) will illustrate in practice all LDA++ methods. In the Sec.IV we will give an example of first-principle calculations of mixed-valence system TmSe and classical Mott insulator NiO within Hubbard-1 approximation to LDA++. Finally we summarize our results in the sec V.

## II. LDA++ METHODS

The ‘‘Kohn-Sham’’ energies of one-particle LDA states cannot be considered as the quasiparticle energies in the sense of many-particle theory (see e.g. [20,21]). In the LDA++ approach they considered only as the ‘‘bare’’ energies and are supposed to be renormalized by the correlation effects. Of course they contain already some part of the correlation effects but only those which may be considered in the local density approximation. The most important ‘‘rest’’ in strongly correlated system is the correlations of the Hubbard type [33] due to the intra-site Coulomb repulsion. Therefore our starting point is the same as in the LDA+U approach. We proceed with the Hamiltonian

$$H = \sum_{ij\sigma\{m\}} t_{m_1 m_2}^{ij} c_{im_1\sigma}^+ c_{jm_2\sigma} + \frac{1}{2} \sum_{i\{\sigma m\}} U_{m_1 m_2 m'_1 m'_2}^i c_{im_1\sigma}^+ c_{im_2\sigma'}^+ c_{im'_2\sigma'} c_{im'_1\sigma} \quad (1)$$

where the  $(i, j)$  represents different crystal sites,  $\{m\}$  label different orbitals and the  $\{\sigma\}$  are spin indices. Coulomb matrix elements are defined in the usual way:

$$U_{m_1 m_2 m'_1 m'_2} = \int \int d\mathbf{r} d\mathbf{r}' \psi_{m_1}^*(\mathbf{r}) \psi_{m_2}^*(\mathbf{r}') V_{ee}(\mathbf{r} - \mathbf{r}') \psi_{m'_1}(\mathbf{r}) \psi_{m'_2}(\mathbf{r}') \quad (2)$$

here  $V_{ee}(\mathbf{r} - \mathbf{r}')$  is the screened Coulomb interactions and  $\psi_m(\mathbf{r})$  are localized on-site basis functions (the site index being suppressed).

In this case all the orbitals are assumed to belong to the ‘‘correlated’’ set, while in real materials like high- $T_c$  compounds (e.g.,  $\text{YBa}_2\text{Cu}_3\text{O}_7$ ) we may define as a first approximation only the 3d orbitals as correlated ones. Therefore it is more reasonable to rewrite Eq.1 in the form of LDA+U Hamiltonian:

$$H = H_{dc}^{LDA} + \frac{1}{2} \sum_{i\{\sigma m\}} U_{m_1 m_2 m'_1 m'_2}^i c_{im_1\sigma}^+ c_{im_2\sigma'}^+ c_{im'_2\sigma'} c_{im'_1\sigma} \quad (3)$$

Note that index  $i$  in the second sum of Eq.3 running only for ‘‘correlated’’ sites, and orbital indices  $\{m\}$  only for ‘‘correlated’’ states (e.g. 3d or 4f) while the first LDA-term:

$$H_{dc}^{LDA} = \sum_{ij\sigma\{m\}} h_{m_1 m_2 \sigma}^{ij} c_{im_1\sigma}^+ c_{jm_2\sigma} - E_{dc}$$

contains all sites and orbitals in the unit cell. Here  $h_{m_1 m_2 \sigma}^{ij}$  are the ‘‘one-particle’’ Hamiltonian parameters in the (spin-polarized) LDA,  $E_{dc}$  is the double counting correction for average Coulomb interactions in L(S)DA [17]:

$$E_{dc} = \frac{1}{2} \bar{U} n_d (1 - n_d) - \frac{1}{2} \bar{J} [n_{d\uparrow} (1 - n_{d\uparrow}) + n_{d\downarrow} (1 - n_{d\downarrow})]$$

with  $\bar{U}$  and  $\bar{J}$  being average Coulomb and exchange interactions and  $n_d = n_{d\uparrow} + n_{d\downarrow}$  is the total number of correlated d(f)-electrons.

One non-trivial problem is to find an efficient way to compute the one electron Hamiltonian  $h^{LDA}$  in a minimal orthogonal basis set. Orthogonality of the basis functions is required for the use of second quantization form of the effective Hamiltonian (Eq.1). Since many-body ( $U$ ) part of the problem is an order of magnitude more time consuming than LDA one, we need to use a minimal basis set and integrated out all high-energy degrees of freedom (out of the  $\pm U$  range). One of the best LDA-methods for such scheme is the Linear Muffin-Tin Orbital (LMTO) method [35], which could give the orthogonal down-folded one-electron tight-binding Hamiltonian. In this case LDA calculations corrected for double counting, produce the first-principle hopping  $t_{ij}$  in many body Hamiltonian.

Now we can describe methods to efficient calculations of quasi-particle (QP) spectra for the LDA+U Hamiltonian. In this sense our approach is not any more density functional theory and one could benefit from the possibility to use the information on QP-band structure comparing with different ‘‘excitation’’ experiments.

## A. Multi-band FLEX

In this section we generalize the FLEX equations [32] for the purpose of multiband LDA++ scheme. We will not take into account a momentum  $\mathbf{q}$ -dependence of the self-energy, although in the FLEX approximation it is straightforward to include it in all the following formulas. The numerical computation of the  $(\mathbf{q}, \omega)$ -dependent self-energy is time-consuming in multiband case [36,37]. To unify the approximations for all our LDA++ schemes we will not include explicitly the  $\mathbf{q}$ -dependence in the FLEX formalism.

First of all one needs to symmetrize the bare vertex matrix  $U$  over different fluctuation channels: particle-hole (density -  $U^d$  and magnetic -  $U^m$ ) and particle-particle (singlet -  $U^s$  and triplet -  $U^t$ ) vertex matrix:

$$\begin{aligned} U_{m_1 m'_1 m_2 m'_2}^d &= 2U_{m_1 m_2 m'_1 m'_2} - U_{m_1 m_2 m'_2 m'_1} \\ U_{m_1 m'_1 m_2 m'_2}^m &= -U_{m_1 m_2 m'_2 m'_1} \\ U_{m_1 m'_1 m_2 m'_2}^s &= \frac{1}{2}(U_{m_1 m'_1 m_2 m'_2} + U_{m_1 m'_1 m'_2 m_2}) \\ U_{m_1 m'_1 m_2 m'_2}^t &= \frac{1}{2}(U_{m_1 m'_1 m'_2 m_2} - U_{m_1 m'_1 m_2 m'_2}) \end{aligned}$$

The one-electron Green-function is defined through the following equation:

$$G_{mm'\sigma}^{-1}(i\omega_n) = (i\omega_n + \mu)\delta_{mm'\sigma} - h_{mm'\sigma} - \Sigma_{mm'\sigma}^{HF} - \Sigma_{mm'\sigma}(i\omega_n)$$

here  $\mu$  is chemical potential,  $\omega_n = (2n+1)/\beta$  are Matsubara frequencies and  $\beta = 1/k_B T$  is inverse temperature. The frequency independent Hartree-Fock part is

$$\Sigma_{mm'\sigma}^{HF} = \sum_{m_1 m_2} (U_{mm_1 m' m_2} \sum_{\sigma'} n_{m_1 m_2}^{\sigma'} - U_{mm_1 m_2 m'} n_{m_1 m_2}^{\sigma}) \quad (4)$$

and corresponds to the rotationally invariant LDA+U method [38].

It is useful to write the multi-band FLEX equations using matrix-vector notation for different Coulomb matrix vertices and vector Green function. We will use a combine index:  $\alpha = \{m, m'\}$  and defined the vector Green function as well as matrix interactions in the following way:

$$\mathbf{G} \equiv \{G_\alpha\}, \quad \widehat{U} = \{U_{\alpha\alpha'}\}$$

For simplicity we first write equations for non-polarized spin states and omit the spin indices. In this case the Hartree-Fock approximation Eq.4 can be rewritten in the form of a matrix-vector product only with ‘‘density’’ Coulomb interaction:

$$\Sigma^{HF} = \widehat{U}^d * \mathbf{n}$$

where the occupation matrix is defined as:

$$n_\alpha \equiv n_{mm'}^\sigma = \langle c_{m\sigma}^\dagger c_{m'\sigma} \rangle = \frac{1}{\beta} \sum_{\omega_n} G_{m'm}(i\omega_n) + \frac{1}{2}\delta_{mm'}$$

Using the single-site Hubbard interactions one obtains a ‘‘local form’’ of FLEX equations in the frequency ( $\omega$ ) - time ( $\tau$ ) space. It is very efficient to use fast-Fourier transforms with periodic boundary condition [39]. Time-frequency spaces are connected by

$$\begin{aligned} \mathbf{G}(i\omega_n) &= \int_0^\beta e^{i\omega_n \tau} \mathbf{G}(\tau) d\tau \\ \mathbf{G}(\tau) &= \frac{1}{\beta} \sum_{\omega_n} e^{-i\omega_n \tau} \mathbf{G}(i\omega_n) \end{aligned}$$

We will try to keep this dual ( $\omega - \tau$ ) notation to stress the numerical implementation of this LDA++ scheme. We write the approximation for self-energy in the ‘‘GW’’-like form :

$$\Sigma(\tau) = \widehat{W}(\tau) * \mathbf{G}(\tau) \quad (5)$$

where symmetrized fluctuation  $W(i\omega)$ -potential defined as:

$$W_{m_1 m_2 m'_1 m'_2} = V_{m_1 m'_1, m'_2 m_2}$$

and total fluctuation potential consists of the second-order term, as well as particle-hole and particle-particle contributions:

$$\widehat{V}(i\omega) = \widehat{V}_2(i\omega) + \widehat{V}_{ph}(i\omega) - \widehat{V}_{pp}(-i\omega)$$

All these contributions can be expressed in terms of bare  $(D_0, M_0, S_0, T_0)$  and renormalized  $(D, M, S, T)$  channel propagators. The second order potential for the non-magnetic case is

$$\widehat{V}_2(i\omega) = \widehat{U} * \widehat{D}_0(i\omega) * \widehat{U}^d \quad (6)$$

while the particle-hole potential is expressed through the density and magnetic fluctuations:

$$\widehat{V}_{ph}(i\omega) = \frac{1}{2} \widehat{U}^d * [\widehat{D}(i\omega) - \widehat{D}_0(i\omega)] * \widehat{U}^d + \frac{3}{2} \widehat{U}^m * [\widehat{M}(i\omega) - \widehat{M}_0(i\omega)] * \widehat{U}^m$$

Finally the particle-particle contribution to fluctuation-exchange potential is:

$$\widehat{V}_{pp}(i\omega) = \widehat{U}^s * [\widehat{S}(i\omega) - \widehat{S}_0(i\omega)] * \widehat{U}^s + 3\widehat{U}^t * [\widehat{T}(i\omega) - \widehat{T}_0(i\omega)] * \widehat{U}^t$$

If one defines the particle-hole ( $\chi$ ) and particle-particle ( $\pi$ ) "empty loop" susceptibilities:

$$\chi_{m_1 m_2 m_3 m_4}(\tau) = -G_{m_4 m_1}(-\tau) * G_{m_2 m_3}(\tau) \quad (7)$$

$$\pi_{m_1 m_2 m_3 m_4}(\tau) = G_{m_1 m_4}(\tau) * G_{m_2 m_3}(\tau)$$

we can write with this notations for susceptibilities the bare channel propagator matrices in the following form for the density and magnetic part:

$$\widehat{D}_0 = \widehat{M}_0 = \widehat{\chi}$$

and for singlet and triplet bare propagators:

$$S_{m_1 m_2 m_3 m_4}^0 = \frac{1}{2} (\pi_{m_1 m_2 m_3 m_4} + \pi_{m_1 m_2 m_4 m_3})$$

$$T_{m_1 m_2 m_3 m_4}^0 = \frac{1}{2} (\pi_{m_1 m_2 m_3 m_4} - \pi_{m_1 m_2 m_4 m_3})$$

The total channel propagators ( $R_\lambda$  where  $\lambda = \{d, m, s, t\}$ ) have to be found from the RPA-like matrix inversion:

$$\widehat{R}_\lambda(i\omega) = [\widehat{1} + \widehat{R}_\lambda^0(i\omega) * U^\lambda]^{-1} * \widehat{R}_\lambda^0(i\omega)$$

The derivation of the complete expression for the FLEX self energy for spin-polarized case with taking into account all the channels are rather cumbersome. Since we will not use here these complicated expressions, they will be discussed in details elsewhere [42].

## B. Hubbard-I approximation

Historically Hubbard-I approximation [33] was the first and the simplest approximations for a strongly correlated one-band model. It has, however, many inconsistencies (see e.g. discussion in [41]). For example it is not conserving (the self energy cannot be represented as a functional derivative of the generating functional with respect to the Green function) and therefore does not obey the Luttinger theorem and other "exact" Fermi-liquid properties. For the half-filled nondegenerate Hubbard model it always gives a gap in the energy spectrum, even for small  $U$ . This means that HIA is completely inapplicable for small and medium interactions. But at the same time it gives a correct picture of the electron spectrum in the narrow-band limit. Therefore it seems to be very useful in 4f systems with a

very strong degree of localization of the electron states. Applying to some real systems in the framework of LDA++ approach, HIA-scheme could give (as it will be shown below) an effective and non-trivial descriptions of many-body multiplet effects.

To introduce Hubbard-I type approximation in degenerate case it is convenient to exploit the so called atomic representation and Hubbard  $X$ -operators (see [43,1,44])

$$X_i^{\mu\nu} = |i\mu\rangle \langle i\nu|$$

where  $\mu, \nu$  are multielectron states of the site  $i$  as a whole (configuration and multiplet indices). In terms of  $X$ -operators the atomic Hamiltonian has very simple form

$$H^{at} = \sum_{\mu} E_{\mu} X^{\mu\mu}$$

On the other hand, the inter-site transfer Hamiltonian, which has very simple (bilinear) structure in terms of the operators  $c_{m'\sigma}^+, c_{m\sigma}$ , also can be expressed in terms of  $X$ -operators by the relations  $c_{m\sigma} = \sum_{\mu\nu} \langle \mu | c_{m\sigma} | \nu \rangle X^{\nu\mu}$  and similarly for  $c_{m'\sigma}^+$ . In the limit of a very strong interaction it is convenient to calculate the Green function via  $X$ -operators (using the decoupling procedure [44] or special diagram technique for  $X$ -operators [40]) and then transform to electron operators. HIA corresponds to the following expression [33,44]:

$$G^{-1}(i\omega) = [G^{at}(i\omega)]^{-1} - \hat{t}$$

where  $\hat{t}$  is the matrix of transfer integrals. In the limit of very small  $\hat{t}$  this expression describes the arising of separate bands from each intraatomic transition with the change of the electron number from unity. It is the picture that seems reasonable for e.g. rare-earth materials with very narrow 4f-band. The bands always appear to be narrowed. Indeed, if in the vicinity of the pole  $i\omega = \varepsilon_0$  the atomic Green function can be represented as

$$G^{at}(i\omega) = \frac{Z_0}{i\omega - \varepsilon_0}$$

the effective transfer Hamiltonian for this ‘‘Hubbard band’’ will be  $Z_0\hat{t}$  instead of  $\hat{t}$ .

In terms of LDA++ multiband approach HIA for Green function has the following form

$$G_{im,jm',\sigma}^{-1}(i\omega) = [(i\omega + \mu)\delta_{mm'} - \Sigma_{mm',\sigma}^{at}(i\omega)] \delta_{ij} - h_{mm',\sigma}^{ij} \quad (8)$$

To obtain this Green function, we need to solve by an exact diagonalization (ED) technique the atomic many-electron problem:

$$H^{at}|v\rangle = E_{\nu}^{at}|v\rangle$$

with the effective atomic Hamiltonian for d- or f-states:

$$H^{at} = \sum_{mm',\sigma} \varepsilon_{mm'} c_{m\sigma}^+ c_{m'\sigma} + \frac{1}{2} \sum_{\{\sigma m\}} U_{m_1 m_2 m'_1 m'_2} c_{im_1\sigma}^+ c_{im_2\sigma}^+ c_{im'_2\sigma'} c_{im'_1\sigma'} \quad (9)$$

Here  $\varepsilon_{mm'}$  is the matrix of atomic energies which in principle can include non-diagonal terms. The latter is naturally come from LMTO-TB effective Hamiltonian which has a diagonal part of  $h_{mm',\sigma}$  as a result of transformation to an orthogonal basis set [35]. Diagonalization of atomic Hamiltonian Eq.9 is not a big problem for a standard workstation, since it is equivalent to 5- and 7-site Hubbard model in ED-scheme [3] for d- and f-states.

Using eigenfunctions and eigenvectors of Hamiltonian (Eq.9, the exact atomic Green-function can be found by the standard definition [20]:

$$G_{mm',\sigma}^{at}(i\omega) = \frac{1}{Z} \sum_{\mu\nu} \frac{\langle \mu | c_{m\sigma} | \nu \rangle \langle \nu | c_{m'\sigma}^+ | \mu \rangle}{i\omega + E_{\mu} - E_{\nu}} (e^{-\beta E_{\mu}} + e^{-\beta E_{\nu}}) \quad (10)$$

where  $Z = \sum_{\nu} e^{-\beta E_{\nu}}$ .

Finally  $\Sigma^{at}$  which is needed for HIA-approximation is found from the following expression:

$$\Sigma_{mm'\sigma}^{at}(i\omega) = i\omega\delta_{mm'} - \varepsilon_{mm'} - (G^{at})_{mm'\sigma}^{-1}(i\omega) \quad (11)$$

Now the HIA-approach to LDA++ may be formulated as a functional for atomic density matrix:  $n_{mm'}$  with a constraint (for  $\varepsilon_{mm'}$ )

$$n_{mm'} = \frac{1}{\beta} \sum_{\omega} G_{mm'}^{at}(i\omega) + \frac{1}{2}\delta_{mm'} \quad (12)$$

(see [20]) having the same  $n_{mm'}$  density matrix for d- or f-electrons as in the crystal as for the corresponding site and orbital element of the Green function, Eq.8.

### C. DMFT-multiband scheme.

A great success of dynamical mean field (d= $\infty$ ) approach to the theory of correlated systems [3] shows that probably this scheme can be the most accurate for the calculations of the self energy from local description of electron fluctuations, at least in the vicinity of the metal-insulator transition. We will use this scheme for real crystals as a best local approximation. The DMFT scheme is based on the "cavity method" or the solution of the effective impurity problem, which corresponds to subtraction of the local self energy only on the one atom in question. In appendix A we show the equivalence of the cavity and impurity methods for matrix multiband Hamiltonians. It was realized recently that the success of DMFT in the one-band half-filled Hubbard model with simplest second-order self-energy is related to the fact that both small and large U-limits are exact in this case [3]. This is not true for non-integer filling or for the multiband case. The elegant iterative perturbation scheme (IPS) for non-integer one-band Hubbard model was proposed recently [45] and gives almost perfect agreement with ED- and QMC-results. For the case of multi-band with non-integer occupations the problem is much more severe and the existing IPS-generalization [46] does not produce good results for large doping. Here we use the main idea of the original IPS-method [45] and propose another version of multiband DMFT which is based more on the numerical solutions of corresponding atomic problem than the approximate analytical one used in [46].

The impurity problem for the "bath" Green function reads:

$$[\mathcal{G}_0(i\omega)]_{mm'}^{-1} = [G(i\omega)]_{mm'}^{-1} + (\mu_0 - \mu)\delta_{mm'} + \Sigma_{mm'}(i\omega)$$

where the local Green function is defined through Brillouin zone sum:

$$G_{mm'}(i\omega) = \frac{1}{N_k} \sum_{\mathbf{k}} G_{mm'}(\mathbf{k}, i\omega)$$

here  $N_k$  is the total number of  $\mathbf{k}$ -points. Alternatively one may perform the  $\mathbf{k}$ -integration using a complex-tetrahedron scheme [47,48]. We introduce here according to [45] the "local" impurity chemical potential  $\mu_0$  to satisfy the condition

$$\sum_{\mathbf{k}} \int_{-\infty}^{+\infty} \frac{d\omega}{2\pi} \text{Tr} \left[ \hat{G}(\mathbf{k}, i\omega) \frac{\partial \hat{\Sigma}(i\omega)}{\partial \omega} \right] = 0$$

which is necessary to provide the Luttinger theorem to be true.

We use the following ansatz for the self energy is in the matrix  $(m, m')$  form:

$$\hat{\Sigma}(i\omega) = \hat{\Sigma}^{HF}(i\omega) + \hat{A} * \hat{\Sigma}^{(2)}(i\omega) * \left[ \hat{1} - \hat{B}(i\omega) * \hat{\Sigma}^{(2)}(i\omega) \right]^{-1} \quad (13)$$

where the second-order self energy  $\hat{\Sigma}^{(2)}(i\omega)$  is defined in terms of the bath Green function  $\mathcal{G}_0(i\omega)$  in according with Eq.5 with  $W = V^{(2)}$  (see also Eq.6):

$$\hat{\Sigma}^{(2)} = \hat{\Sigma}^{(2)}[\mathcal{G}_0]$$

In spirit of the approach [45] the  $A$ -matrix should be defined to provide the exact high-energy ( $\omega \rightarrow \infty$ ) limit of  $\hat{\Sigma}(i\omega)$ . The best way to receive such asymptotic is the using of the equations of motion for the double-time retarded Green function with the analytical continuation on the Matsubara frequencies [20,40]. One has exact at  $\omega \rightarrow \infty$  expression

$$\Sigma_{mm'\sigma}(i\omega) = \frac{1}{i\omega} N_{mm'\sigma}$$

where

$$N_{mm'\sigma} = \langle \{ [c_{m\sigma}, H_{int}], [H_{int}, c_{m'\sigma}^+] \} \rangle$$

here  $[\dots, \dots]$  and  $\{\dots, \dots\}$  are the symbols for commutator and anticommutator, correspondingly,  $H_{int}$  is the Hubbard (interaction) part of the Hamiltonian. Note that in the multiband case the average  $N_{mm'\sigma}$  contains the products of four electron operators and cannot be found exactly. Decoupling of these four-fermion averages according to the Wick theorem and comparing the result with the asymptotic of  $\widehat{\Sigma}^{(2)}$ :

$$\Sigma_{mm'\sigma}^{(2)}(i\omega \rightarrow \infty) = \frac{N_{mm'\sigma}^0}{i\omega}$$

we obtain the following expression

$$\widehat{A} = \widehat{N} * [\widehat{N}^0]^{-1}$$

where  $\widehat{N}_0$ -matrix defined in the spin-polarized case as:

$$N_{mm'\sigma}^0 = \sum_{\{m_i\}} \{ U_{mm_3m_1m_4} U_{m_1m_5m'm_2} \sum_{\sigma'} n_{m_5m_4\sigma'}^0 (\delta_{m_3m_2} - n_{m_3m_2\sigma'}^0) \\ - U_{mm_3m_4m_1} U_{m_1m_5m'm_2} n_{m_5m_4\sigma'}^0 (\delta_{m_3m_2} - n_{m_3m_2\sigma}^0) \}$$

and in the non-magnetic case it simplifies to:

$$N_{mm'}^0 = \sum_{\{m_i\}} U_{mm_1m_3m_4}^d U_{m_1m_5m'm_2} n_{m_5m_4}^0 (\delta_{m_3m_2} - n_{m_3m_2}^0)$$

The expression for  $\widehat{N}$ -matrix differing from that for  $\widehat{N}^0$  by the replacement of the occupation matrix  $n^0 \rightarrow n$ . Note that matrix  $\widehat{A}$  appears to be non-Hermitian. In the non-degenerate case this expression appears to be exact (see [45]) due to the identity

$$(c_{m\sigma}^+ c_{m\sigma})^2 = c_{m\sigma}^+ c_{m\sigma}.$$

It can be quite accurate also in the general multiband case.

Coefficient matrix  $\widehat{B}$  is designed to fix the exact atomic limit of the interaction self energy, Eq.13. There are other problems with coefficient  $B$  in the multiband case [46]. While in single band model one can find an analytical expression for the constant  $B$  [45], in the multiband case this parameter should be  $\omega$ -dependent, owing to the frequency dependence of the atomic self-energy, Eq.11. We decide to find numerically the non-Hermitian matrix  $B(i\omega)$  from atomic limit of Eq.13 using the exact  $\widehat{\Sigma}_{at}(i\omega)$  with a constraint for the density matrix  $\widehat{n}$ . In this limit  $\widehat{\Sigma}^{(2)}(i\omega)$  in the non-magnetic case has the form:

$$\widehat{\Sigma}_{mm'}^{(2)at}(i\omega) = \sum_{\{m_i\}} U_{mm_1m_3m_2}^d U_{m_1m_2m'm_3} \frac{[f_{m_3}(1 - f_{m_2} - f_{m_1}) + f_{m_1}f_{m_2}]}{i\omega + \mu_0 - \varepsilon_{m_2} + \varepsilon_{m_3} - \varepsilon_{m_1}}$$

here  $f_{m_i}$  and  $\varepsilon_{m_i}$  are diagonal occupation numbers and energies of  $h^{at}$ . In this case we have:

$$\widehat{B}(i\omega) = [\widehat{\Sigma}^{(2)at}(i\omega)]^{-1} - [\widehat{\Sigma}^{at}(i\omega) - \widehat{\Sigma}^{HF}]^{-1} * \widehat{A} \quad (14)$$

As a simple example for such scheme we compare on Fig.1 DMFT to exact-diagonalization for the Anderson model of two-site, two-bands with one correlated site  $U = 4$ ,  $\varepsilon_f = -4$  and one “free-site” with  $\varepsilon_0 = 0$  and hybridization between the sites  $V = 0.25$  [46]. For convenient we assume that all parameters for our model calculations are in “eV” energy units. The corresponding Hamiltonian for Anderson impurity model has the following form:

$$H_{imp} = \varepsilon_f \sum_{m\sigma} f_{m\sigma}^+ f_{m\sigma} + V \sum_{m\sigma} (f_{m\sigma}^+ c_{m\sigma} + c_{m\sigma}^+ f_{m\sigma}) + U \sum_m f_{m\uparrow}^+ f_{m\uparrow} f_{m\downarrow}^+ f_{m\downarrow}$$

It is not a problem to find an exact Green function for this model (non-symmetrize many-body Hamiltonian has the dimension  $256 \times 256$ ) and compare with approximate calculations. We see that the agreement between exact solution and our DMFT results is quite good even for a large filling ( $n_{tot} > 1$ ; in this case  $n_f = 0.76$ ,  $n_{tot} \approx 2$ ). Also note that the atomic Green-function in Fig.1 for correlated site has the “three-peak” structure for this occupations (there are general 8 poles in Green-functions for two-band case) and not the two-peak structure as in the one-band model. The use of the *numerical* atomic Green function for the  $B(i\omega)$ -matrix calculation is quite important even for qualitative agreement with exact results for such model at the filling larger than one electron per site [45]

### III. RESULTS FOR TWO-BAND MODEL.

In this section we compare the three different LDA++ approaches described above for a two-band system. We used the simplified two-dimensional model for High-Tc superconductors for  $d_{x^2-y^2} \equiv x$  and  $d_{z^2} \equiv z$  orbitals [34]. If one can skip  $z$ -orbital it will be standard single-band nearest neighbor hopping (“t”)-model. LDA band structure calculation for High-Tc materials shows the large contribution of Cu  $d_{z^2}$  orbital to states near the Fermi level [49]. Therefore the situation with two correlated valence bands could be possible in this materials. Although we knew that for the realistic description of Cu  $d_{x^2-y^2}$  state in single band model one need to include next-nearest hoppings (coming from interactions with O2p- and Cu4s-orbitals [49]) we used here the simplified tight-binding model for two correlated bands “x” and “z” within nearest-neighbour hopping approximation. The one electron Hamiltonian has the following form [34]:

$$\hat{h}(\mathbf{k}) = \begin{pmatrix} -2t_{xx}(\cos k_x + \cos k_y) + \Delta, & -2t_{xz}(\cos k_x - \cos k_y) \\ -2t_{xz}(\cos k_x - \cos k_y), & -2t_{zz}(\cos k_x + \cos k_y) \end{pmatrix}$$

The hopping parameters are related via simple Slater-Koster ratio:  $t_{xx} = 1$ ,  $t_{zz} = 0.3$ ,  $t_{xz} = 0.4$ . Again we assume that all TB-parameters are in “eV” energy units, while the value  $t_{xx} \sim 0.5$  eV would be more realistic [49]. It is important to take into account the energy shifting parameter  $\Delta$  since Cu  $d_{x^2-y^2}$  bands located higher than Cu  $d_{z^2}$ -one, so we use  $\Delta = 4$ . For the Coulomb energy our parameterization corresponds to the following matrix elements ( $m_1 \neq m_2$ ):  $U_{m_1 m_1 m_1 m_1} = U + J$ ,  $U_{m_1 m_2 m_1 m_2} = U$ ,  $U_{m_1 m_2 m_2 m_1} = J$ , and  $U_{m_1 m_2 m_1 m_1} = \delta J$ . In this case the symmetrized bare vertices has the following form (the basis function numbering as:  $xx, xz, zx, zz$ ):

$$U^d = \begin{pmatrix} U + J & \delta J & \delta J & 2U - J \\ \delta J & 0 & 2J - U & \delta J \\ \delta J & 2J - U & 0 & \delta J \\ 2U - J & \delta J & \delta J & U + J \end{pmatrix}, \quad U^m = \begin{pmatrix} -U - J & -\delta J & -\delta J & -J \\ -\delta J & 0 & -U & -\delta J \\ -\delta J & -U & 0 & -\delta J \\ -J & -\delta J & -\delta J & -U - J \end{pmatrix}$$

$$U^s = \begin{pmatrix} U + J & \delta J & \delta J & 0 \\ \delta J & \frac{1}{2}(J + U) & \frac{1}{2}(J + U) & \delta J \\ \delta J & \frac{1}{2}(J + U) & \frac{1}{2}(J + U) & \delta J \\ 0 & \delta J & \delta J & U + J \end{pmatrix}, \quad U^t = \begin{pmatrix} 0 & 0 & 0 & 0 \\ 0 & \frac{1}{2}(J - U) & \frac{1}{2}(J - U) & 0 \\ 0 & \frac{1}{2}(J - U) & \frac{1}{2}(J - U) & 0 \\ 0 & 0 & 0 & 0 \end{pmatrix}$$

We investigate this model for different  $U$  parameters:  $U = 2 - 8$  with the fixed values of  $J = 0.5$  and  $\delta J = 0.1$ . The total number of electrons are  $n_{tot} = 1.4$  which approximately corresponds to fully occupied  $z$ -bands and almost half-field  $x$ -band with 10% of holes. We use the  $32 \times 32$  mesh for the summation over the Brillouin zone and 4000 – 8000 Matsubara frequencies with the cutoff energy equals to 20 – 40 times the bandwidth. On the Fig.2 we show the results of self-consistent FLEX two-band calculations for  $U = 2, 4, 6$  and 8. Density of state (DOS) was obtained from the Green function, extrapolating Matsubara frequencies with Pade approximation [50] to the real axis. Note that the bare bandwidth for  $t_{xz} = 0$  is equal to  $8t$  in the case of two dimensional square lattice and corresponds to 8 and 2.4 eV for  $x$  and  $z$  bands. One can see the narrowing the DOS-peak near Fermi energy ( $E_F$ ) for  $x$ -band and boarding the total  $x$ - and  $z$ - subbands as  $U$  increased. An interesting feature of this two-band model is seen in moving the peak from occupied  $z$ -band towards the Fermi level with increasing correlation strength  $U$ , and a pinning of the van-Hove peak from the  $x$ -band just above Fermi level. This drastic change of the  $x$ - and  $z$ - band-shape maximize the particle-hole interband susceptibility (inversely proportional to the energy distance between band peaks) and therefore increase the fluctuation contribution to FLEX-energy. The value of the average inverse mass enhancement factor  $Z = [1 - \partial \Sigma(\epsilon) / \partial \epsilon]_{\epsilon=0}^{-1}$  is equal to 0.45 and 0.83 for  $x$  and  $z$  orbitals for  $U=4$ . Spectral function  $A(\mathbf{k}, \epsilon) = -1/\pi \text{Tr} \text{Im} G(\mathbf{k}, \epsilon)$  for three different  $\mathbf{k}$ -directions in two-dimensional Brillouin zone is shown in Fig.3. One could see the renormalized dispersion of two bands:  $x$ -band from approximately -5 eV at X-point to 5 eV at M-point and  $z$ -band from approximately -8 eV at X-point to 3 eV at M-point. Similar to all High- $T_c$  models [36] there is an extended van-Hove singularity in  $x$ -bands just at the Fermi energy near X-point.

The results of self-consistent DMFT calculations for  $U = 4$  and  $8$  are presents in Fig.4. In this case we use only first seven Matsubara frequencies in the Eq.14 and the constant B-matrix for the rest frequencies. One can clearly see some differences to the corresponding FLEX results, which is related to a sharpness of the DOS near  $E_F$  and more pronounced three peak structure of partial  $x$ -band DOS for  $U=8$ . We plot also the DOS corresponding to the atomic Green function for  $U=8$  with the four poles near to Fermi energy out of eight poles in the paramagnetic two-orbital atom. Corresponding spectral function for the same directions in Brillouin zone is presents in the Fig.5 for  $U=8$ . There is a sharp quasiparticle dispersion near the Fermi level and broad incoherent background above  $E_F$  at the energy of about 7 eV near M-point. Extended van-Hove singularity at X-point become more pronounced. We plot also the momentum distribution function  $n(\mathbf{k})$  in (1,1) direction in the Fig.6. From the quasiparticle dispersion of the  $x$ -band along  $\Gamma - M$  direction (Fig.5), we expect the Fermi surface crossing almost exactly at the half-way between this two points. The momentum distribution function (Fig.6) just confirm this situations and shows that the Fermi step (our simulation temperature  $T=0.06t$ ) is smaller than one and agree with the calculated value of the mass renormalization factor  $Z=0.43$  for  $x$ -band.

Finally the HIA-solution for this two-band model for  $U = 8$  is shown in Fig.7. In this case we have the dielectric DOS with narrow atomic-like resonances. It is interesting to mention that the structure of the atomic Green function in the DMFT approximation (Fig.4) quite close to the HIA-solution shifted approximately by 2 eV down. We would like to mention that the application of HIA-scheme is reasonable only for  $U \gg W$  and not for  $U=W$  as in this case.

#### IV. LDA++ CALCULATIONS FOR REAL SYSTEMS

The self-consistent LDA++ calculation for real systems pose a serious computational problem. One need to operate with the susceptibility matrix, which is of dimension  $N_d^2 \times N_d^2$  and depends on the Matsubara frequencies. For a illustrative purpose we have calculated the electronic structure of classical Mott-Hubbard insulator NiO and mixed valence 4f-compound TmSe in HIA scheme for LDA++. We use non-selfconsistent HIA approximation with the simplest constrain for only diagonal  $\varepsilon_f$  in Eq.9 to have  $n_d$  for NiO or  $n_f$  electrons for TmSe from self-consistent paramagnetic LDA-calculations. The Coulomb matrix is expressed via effective Slater integrals:

$$U_{m_1 m_2 m'_1 m'_2} = \sum_k a_k(m_1, m'_1, m_2, m'_2) F^k$$

where  $0 \leq k \leq 2l$  and

$$a_k(m_1, m'_1, m_2, m'_2) = \frac{4\pi}{2k+1} \sum_{q=-k}^k \langle l m_1 | Y_{kq} | l m'_1 \rangle \langle l m_2 | Y_{kq}^* | l m'_2 \rangle$$

We used the following effective Slater parameters, which define screened Coulomb interaction in d-shell for NiO:  $F^0 = 8.0$  eV,  $F^2 = 8.2$  eV,  $F^4 = 5.2$  eV, and in f-shell for TmSe:  $F^0 = 5.7$  eV,  $F^2 = 9.1$  eV,  $F^4 = 5.7$  eV,  $F^6 = 4.7$  eV, (see e.g. [16,51,52]). We start from the non-magnetic LDA calculations in the LMTO nearly-orthogonal representation [35] for experimental crystal structures of NiO and TmSe. The minimal basis set of  $s, p, d$ -orbitals for NiO and  $s, p, d, f$ - orbitals for TmSe corresponds to  $18 \times 18$  and  $32 \times 32$  matrix of the LDA Hamiltonian  $h(\mathbf{k})$ . The occupation number for correlated electrons are 8.4 electrons in the d-shell of Ni and 12.6 electrons if the 4f-shell of Tm. Using the corresponding atomic self energy for Ni-atom and Tm-atom the total DOS for NiO and TmSe have been calculated from Eq.8. In Fig.8 we compare the paramagnetic LDA results with HIA LDA++ scheme. It is well known that paramagnetic LDA calculations can not produce the insulating gap in nickel oxide: the Fermi level located in the middle of the half-filled  $e_g$  bands [18]. In the HIA approximation to LDA++ approach there is a gap (or pseudogap in the Fig8 due to temperature broadening) of the order of 3.5 eV even in this “nonmagnetic” state. This gap and the satellites at -5 and -8 eV are related to the structure of atomic Green function shown in the lower panel of the Fig.8.

In Fig.9 we compare the calculated DOS for TmSe with experimental XPS spectrum [53]. The HIA approximation in this case well reproduces the ladder-type photoemission spectrum, comes mainly from combinations of two multiplets structure of  $Tm^{2+}(f^{13})$  and  $Tm^{3+}(f^{12})$ . This example demonstrate how the LDA++ scheme can combine the many-body atomic physics with band structure methods. Normal LDA-band structure for rare-earth systems corresponds to the narrow f-peak at the Fermi level and could not describe the experimental XPS-spectrum which has the “f”-resonances over wide energy range of the order of 12 eV. At the same time, HIA is not adequate to describe correctly the fine features of the electron structure near the Fermi level. It is known [54] that TmSe is really the narrow-gap semiconductor. According to the most developed model approach to mixed-valence semiconductors [55,1] the appearance of this energy gap is caused by both hybridization and exciton effects due to the Coulomb attraction of 5d

conduction electron and 4f hole. This effect cannot be described in HIA approximation. Nevertheless we believe that the description of the electronic structure of f compounds including mixed-valence ones on the large energy scales is important itself and in this sense the results presented here demonstrate the usefulness of LDA++ approach for the description of real strongly correlated systems.

## V. SUMMARY

We have formulate a general LDA++ scheme which takes into account dynamical electron fluctuations in the case of correlated d- or f-states. The most accurate approach is the DMFT-band structure method, while more simple FLEX and HIA scheme can be as well useful for investigation of correlation effects in real systems, in the cases of rather weak and rather strong interaction respectively. In principle one could combine the idea of the bath-Green function in DMFT-scheme with the simple expression for the self-energy in the FLEX approximation. In this case  $\hat{\Sigma} = \hat{\Sigma}^{FLEX}[\mathcal{G}_0]$  and we expected effectively reduce the effects of vertex-corrections in the FLEX scheme.

Here we compare the LDA++ approach with more simple LDA+U one. First of all, to describe Mott insulators in LDA+U approach (as well as in SIC approach) it is necessary to assume magnetic and (or) orbital ordering [18]. In LDA++ it is possible to consider the *paramagnetic* Mott insulators in the framework of *ab initio* calculations. Moreover, it is possible to obtain not only the Mott-Hubbard gap in the electron spectrum but also satellites and multiplet structure (see e.g. the results for TmSe and NiO in the previous Section).

The correlation effects results from the frequency dependence of the self energy ( the non-Fermi-step form of the distribution function for quasiparticles, the mass enhancement, the appearance of many-electron Kondo resonances etc) can be obtained and investigated in LDA++ approach but not in LDA+U. Our results for two-band model provide the interesting examples of such behavior. In particular it is worthwhile to note such features as the narrowing of the van Hove singularity and its “pinning” to the Fermi level (which is important for the physics of High Tc superconductors [36] and can be described already in multiband FLEX approximation), the “three-peak” structure of the spectrum in the vicinity of Mott insulators (“Kondo resonance” and mid-gap states which can be described in DMFT approach).

We hope that the approximations described here may be useful for the *ab initio* calculations of electron structure of a great variety of strongly correlated electron systems including doped Mott insulators, rare-earth metals and their compounds (in particular mixed-valence ones), high-temperature superconductors and many others.

## VI. ACKNOWLEDGEMENTS

Part of this work has been carried out during the visit of one of the author (MIK) to the Max-Planck-Institute of Solid State (Stuttgart), Max-Planck-Institute of Physics of Complex Systems (Dresden), and Forschungszentrum Jülich. The authors are grateful to Max-Planck Society and Forschungszentrum Jülich and benefit a lot from discussions with O.K. Andersen, V.I. Anisimov, A.O. Anokhin, P. Fulde, O. Gunnarsson, L. Hedin, P. Horsh, and G. Kotliar.

## VII. APPENDIX A

Here we present the proof of the equivalence of a “cavity method” and impurity problem in DMFT for multiband case. We start with the expression for the Green function matrix on the zero site in the cavity method (see [3], Eq.(35))

$$[\mathcal{G}_0(i\omega)]^{-1} = i\omega + \mu - h_{at} - R,$$

where

$$R = \sum_{ij} t_{0i} G_{ij}^{(0)} t_{j0} \quad (15)$$

with  $h_{at}$  being the one-electron part of the intra-atomic Hamiltonian. All this functions are the matrix in  $(m, m')$  indices as well as diagonal matrix in spin-space. Note that  $G_{ij}^{(0)}$  is the Green function between sites  $i$  and  $j$  on the lattice with the site zero being eliminated

$$G_{ij}^{(0)} = G_{ij} - G_{i0} G_{00}^{-1} G_{0j} \quad (16)$$

Using the Fourier expansion of all the quantities over the Brillouin zone and substituting Eq.16 to Eq.15 one has

$$R = M - LG_{00}^{-1}L^T$$

where

$$L = \sum_i t_{0i}G_{i0} = \sum_{\mathbf{k}} t(\mathbf{k})G(\mathbf{k})$$

and

$$M = \sum_{ij} t_{0i}G_{ij}t_{j0} = \sum_{\mathbf{k}} t(\mathbf{k})G(\mathbf{k})t(\mathbf{k})$$

At the same time (see [3])

$$G(\mathbf{k}) = [\Lambda - t(\mathbf{k})]^{-1}$$

$$\Lambda = i\omega + \mu - h_{at} - \Sigma(i\omega) \tag{17}$$

Taking into account that  $\sum_{\mathbf{k}} t(\mathbf{k}) = 0$  one obtains

$$L = \sum_{\mathbf{k}} [t(\mathbf{k}) - \Lambda + \Lambda] [\Lambda - t(\mathbf{k})]^{-1} = -1 + \Lambda G_{00}$$

and

$$L^T = -1 + G_{00}\Lambda$$

One can obtain by the similar way the result for M-matrix:  $M = \Lambda L^T$   
Substituting all this formulas to Eq.15 we have

$$R = (\Lambda + G_{00}^{-1} - \Lambda)L^T = -G_{00}^{-1} + \Lambda$$

using Eq.17, we can finally write:

$$[\mathcal{G}_0(i\omega)]^{-1} = i\omega + \mu - h_{at} - \Lambda + G_{00}^{-1} = \Sigma(i\omega) + G_{00}^{-1}$$

It means that  $\mathcal{G}_0(i\omega)$  is the Green function of the impurity problem with the on-site one-electron Hamiltonian  $h_{at} + \Sigma(i\omega)$  on each “non-zero” site and  $h_{at}$  for zero site.

- [1] S.V. Vonsovskii, M.I. Katsnelson, and A.V. Trefilov, Phys. Metals Metallogr. **76**, 247, 343 (1994).
- [2] P.W. Anderson, *50 years of the Mott phenomenon*. In: Frontiers and Borderlines in Many Particle Physics, eds. J.R. Schrieffer and R.A. Broglia, North-Holland, Amsterdam, 1988.
- [3] A. Georges, G. Kotliar, W. Krauth, and M. Rozenberg, Rev. Mod. Phys. **68**, 13 (1996).
- [4] D.J. Scalapino, Phys. Rep. **251**, 1 (1994).
- [5] P. Hohenberg and W. Kohn, Phys. Rev. **136**, B864 (1964).
- [6] R.O. Jones and O. Gunnarsson, Rev. Mod. Phys. **61**, 689 (1989).
- [7] E.K.U. Gross and W. Kohn, Phys. Rev. Lett. **55**, 2850 (1985), M. Petersilka, U.J. Gossmann, and E.K.U. Gross, Phys. Rev. Lett. **76**, 1212 (1996).
- [8] A. Felzar, A.A. Quong, and A.G. Eguiluz, Phys. Rev. Lett. **74**, 590 (1995).
- [9] L.Mitás and R. Martin, Phys. Rev. Lett. **72**, 2438 (1994).
- [10] S. Tanaka, J. Phys. Soc. Japan, **64**, 4270 (1995).
- [11] R.Q. Hood, M.Y. Chou, A.J. Williamson, G. Rajagopal, R.J. Needs and W.M.C. Foulkes, Phys. Rev. Lett. **78**, 3350 (1997).
- [12] L. Hedin, Phys. Rev. **139**, A796 (1965).

- [13] F. Aryasetiawan and O. Gunnarsson, Phys. Rev. Lett. **74**, 3221 (1995).
- [14] A. Seidl, A. Görling, P. Vogl, J.A. Majewski, and M. Levy, Phys. Rev. B. **53**, 3764 (1996); H. Rücker, to be published.
- [15] G.E. Engel, Phys. Rev. Lett. **78**, 3515 (1997).
- [16] V.I. Anisimov, J. Zaanen and O.K. Andersen, Phys. Rev. B. **44**, 943 (1991).
- [17] V.I. Anisimov, I.V. Solovyev, M.A. Korotin, M.T. Czyzyk, and G.A. Sawatzky, Phys. Rev. B. **48**, 16929 (1993).
- [18] V.I. Anisimov, F. Aryasetiawan, and A.I. Lichtenstein, J. Phys.: Condens. Matter, **9**, 767 (1997).
- [19] A.Svane and O.Gunnarsson, Phys. Rev. Lett. **65**, 1148 (1990).
- [20] A.A. Abrikosov, L.P. Gorkov, and I.E. Dzialoshinskii, *Methods of Quantum Field Theory in Statistical Physics*, Pergamon, New York, 1965.
- [21] G. Mahan, *Many-Particle Physics*, Plenum Press, New York, 1981.
- [22] A.I. Lichtenstein and M.I. Katsnelson, Bull. Am. Phys. Soc., **42**, 573 (1997).
- [23] L. Kleinman and K. Mednick, Phys. Rev. B. **24**, 6880 (1981).
- [24] G. Tréglia, F. Ducastelle, and D. Spanjaard, J. Phys (Paris) **43**, 341 (1982).
- [25] M.M. Steiner, R.C. ALbers, and L.J. Sham, Phys. Rev. B. **45**, 13272 (1992).
- [26] M.M. Steiner, R.C. ALbers, and L.J. Sham, Phys. Rev. Lett. **72**, 2923 (1994).
- [27] I.S. Sandalov, O. Hjortstam, B. Johansson, and O. Erikson, Phys. Rev. B. **51**, 13987 (1995).
- [28] F. Manghi, C. Calandra, and S. Ossicini, Phys. Rev. Lett. **23**, 3129 (1994).
- [29] M. Takahashi and J. Igarashi, Phys. Rev. B. **54**, 13566 (1996).
- [30] F. López-Aguilar, J. Costa-Quintana, and L. Puig-Puig, Phys. Rev. B. **48**, 1128 (1993), **48**, 1139 (1993), **54**, 10265 (1996).
- [31] J.E. Han, M. Alouani, and D.L. Cox, Phys. Rev. Lett. **78**, 939 (1997).
- [32] N.E. Bickers and D.J. Scalapino, Annals of Physics, **193**, 206 (1989).
- [33] J.Hubbard, Proc.Roy.Soc., **A276**, 238 (1963); **A277**, 237 (1964)
- [34] F. Buda, D.L. Cox, and M. Jarell, Phys. Rev. B. **49**, 1255 (1994).
- [35] O.K. Andersen, O. Jepsen, and G. Krier, in: *Lectures on Methods of Electronic Structure Calculations*, eds. V. Kumar, O.K. Andersen and A. Mookerjee, World Scientific, 1994, p. 63.
- [36] A.I. Lichtenstein, O. Gunnarsson, O.K. Andersen, and R.M. Martin, Phys. Rev. B. **54**, 12505 (1996).
- [37] R. Putz, R. Preuss, A. Muramatsu and W. Hanke, Phys. Rev. B. **53**, 5133 (1996).
- [38] A.I. Lichtenstein, J. Zaanen, V.I. Anisimov, Phys. Rev. B. **52**, R5426 (1995).
- [39] J.W. Serene, et. al. Phys. Rev. B. **44**, 3391 (1991).
- [40] Yu.A. Izyumov, M.I. Katsnelson, and Yu.N. Skryabin, *Magnetism of Itinerant Electrons*, Nauka, Moscow, 1994.
- [41] F. Gebhard, *The Mott Metal-Insulator Transition*, Springer, Berlin, 1997.
- [42] M.I. Katsnelson and A.I. Lichtenstein, to be published.
- [43] J.Hubbard, Proc.Roy.Soc., **A285**, 542 (1965)
- [44] V.Yu.Irkhin, Yu.P.Irkhin, Phys. Stat. Sol. (b) **183**, 9 (1994)
- [45] H. Kajueter and G. Kotliar, Phys. Rev. Lett. **77**, 131 (1996); H. Kajueter, PhD Thesis, Rutgers University, 1996.
- [46] H. Kajueter and G. Kotliar, Int. J. Mod. Phys. B. **11**, 729 (1997).
- [47] Ph. Lambin and J.P. Vigneron, Phys. Rev. B. **29**, 3430 (1984).
- [48] V.I. Anisimov, A.P. Poteryaev, M.A. Korotin, A.O. Anokhin, and G. Kotliar, cond-mat/9704231.
- [49] O.K. Andersen, A.I. Lichtenstein, O. Jepsen and F. Paulsen, J. Phys. Chem. Solids, **56**, 1573 (1995).
- [50] H.J. Vidberg and J.W. Serene, J. Low Temp. Phys., **29**, 179 (1977).
- [51] D. van der Marel and G.A. Sawatzky, Phys. Rev. B. **37**, 10674 (1988).
- [52] B.L. Thole, G. van der Laan, J.C. Fuggle, and G. A. Sawatzky, Phys. Rev. B. **32**, 5107 (1988).
- [53] M. Campagna, G.K. Wertheim, and E. Bucher, *Structure and Bonding*, v.**30**, p. 99, Springer, 1976.
- [54] P. Wachter, J. Magn. Magn. Mater., **31-34**, 439 (1985); A. Amato and J. Sierro, J. Magn. Magn. Mater., **47-48**, 475 (1985).
- [55] V.Yu. Irkhin and M.I. Katsnelson, Zh.Eksp.Teor.Fiz. **90**, 1080 (1986); Fizika Tverd. Tela **29**, 1461 (1987).

FIG. 1. Energy spectrum for two-band two-site Anderson model in exact diagonalization and DMFT scheme as well as atomic green function for correlated cite.

FIG. 2. Density of states for two band model in the FLEX scheme for different U-values. Full and dashed lines indicate partial DOS for  $x$ - and  $z$ - orbitals.

FIG. 3. Spectral function (the two band FLEX model,  $U=4$ ) for three different directions in the two-dimensional square Brillouin zone:  $\Gamma = (0, 0)$ ,  $X = (0.5, 0)$ , and  $M = (0.5, 0.5)$  in units of  $2\pi/a$ .

FIG. 4. Density of states for two band model in the DMFT scheme for different U-values as well as atomic Green function for  $U=8$ . Full and dashed lines indicate partial DOS for  $x$ - and  $z$ - orbitals.

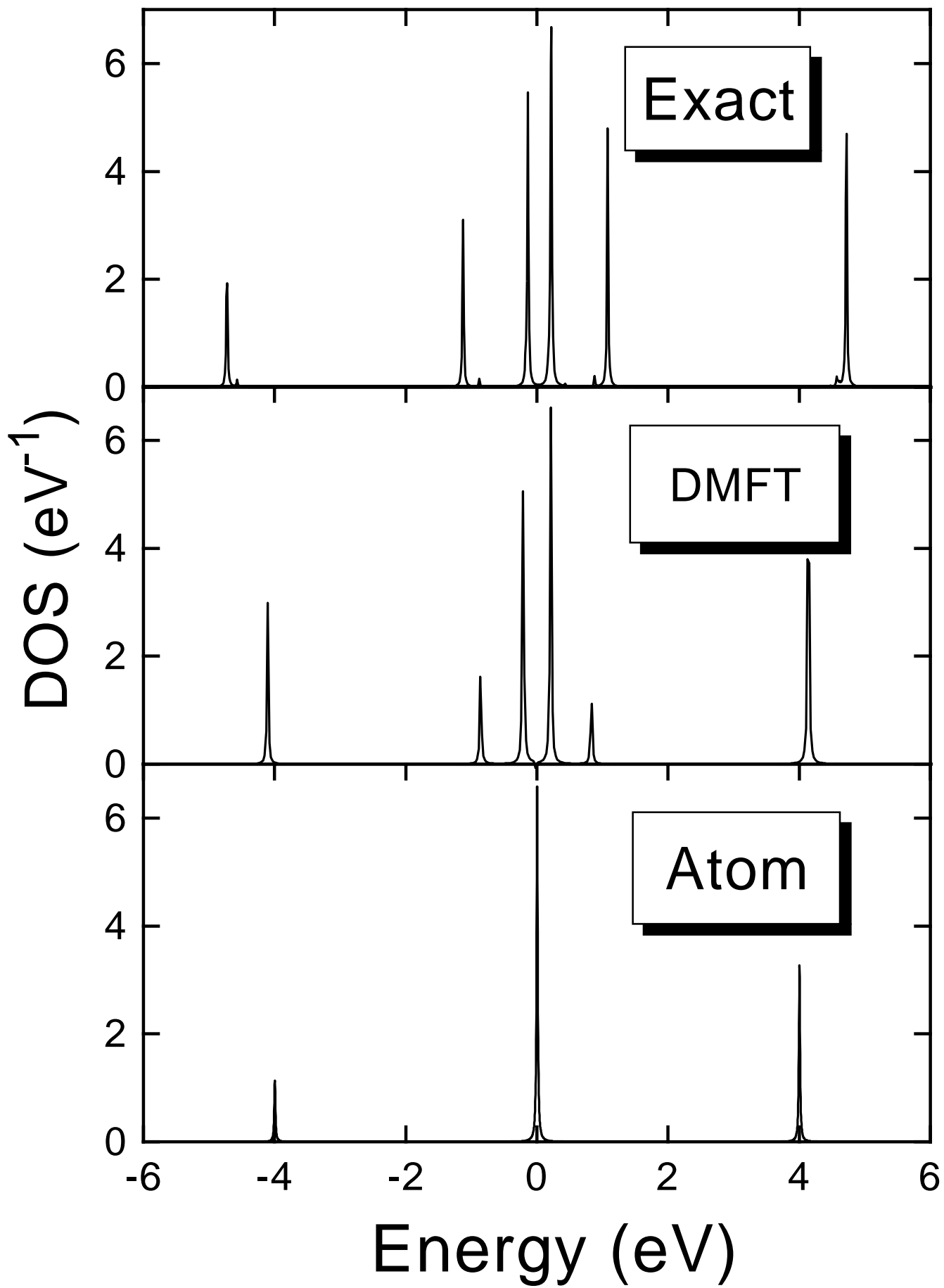
FIG. 5. Spectral function (the two band DMFT model  $U=8$ ) for three different direction in the two-dimensional square Brillouin zone

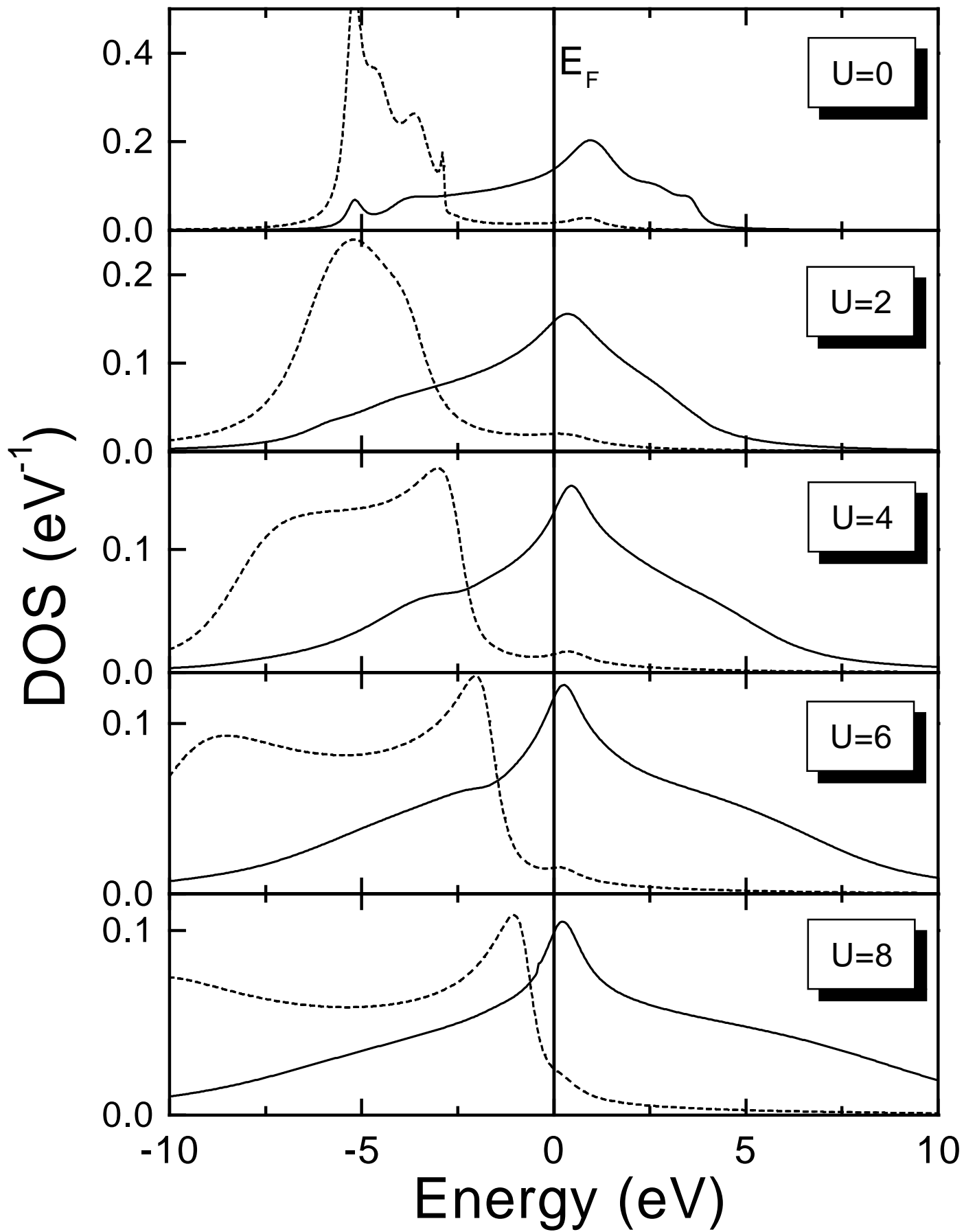
FIG. 6. The momentum distribution function  $n(\mathbf{k})$  in  $(1,1)$  direction for the two band DMFT model  $U=8$ .

FIG. 7. Density of states for two band model in the HIA scheme for  $U=8$ . Full and dashed lines indicate partial DOS for x and z orbitals.

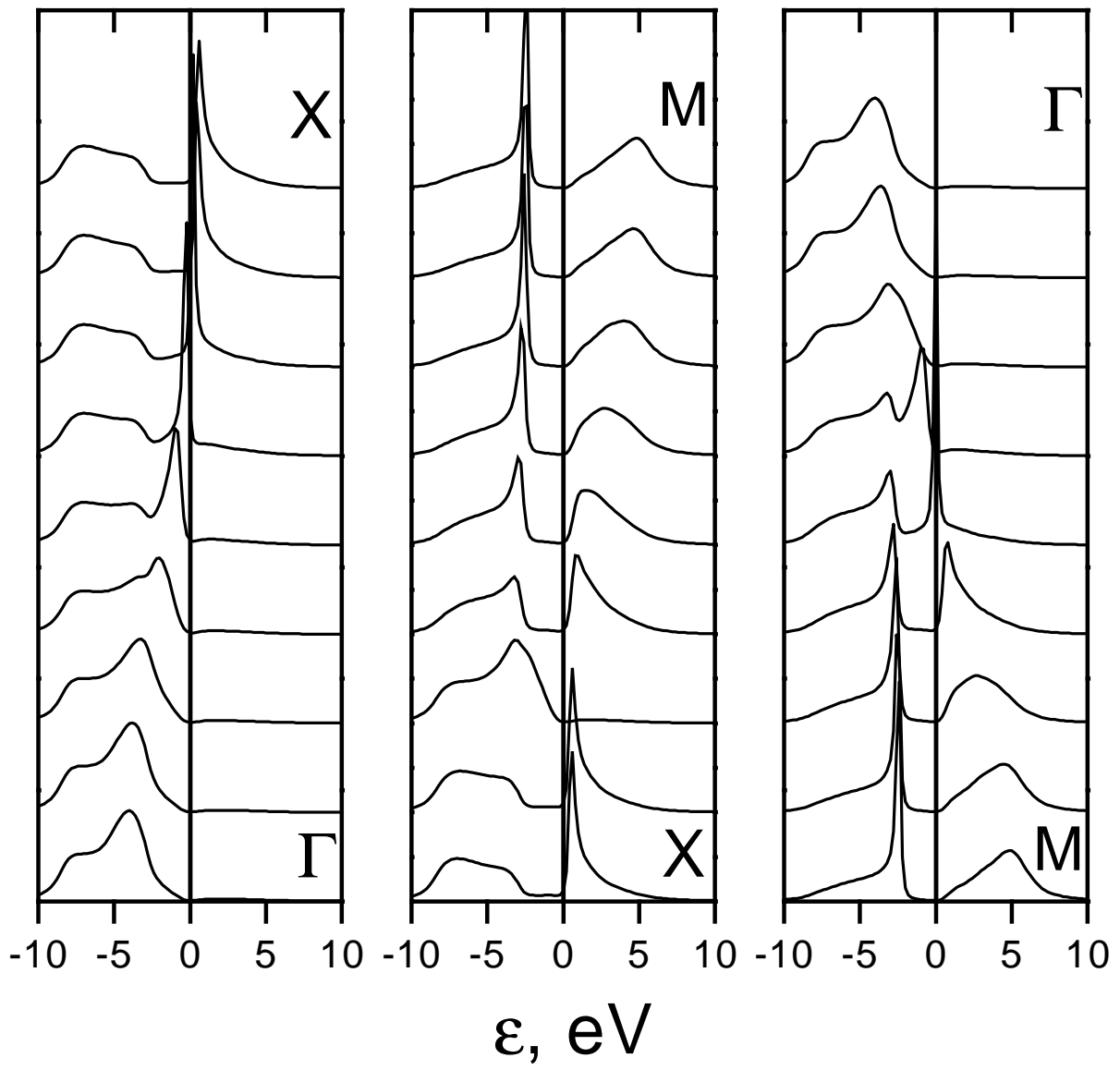
FIG. 8. Density of states for paramagnetic nickel oxide in the LDA and HIA approximations as well as Ni-atom Green function.

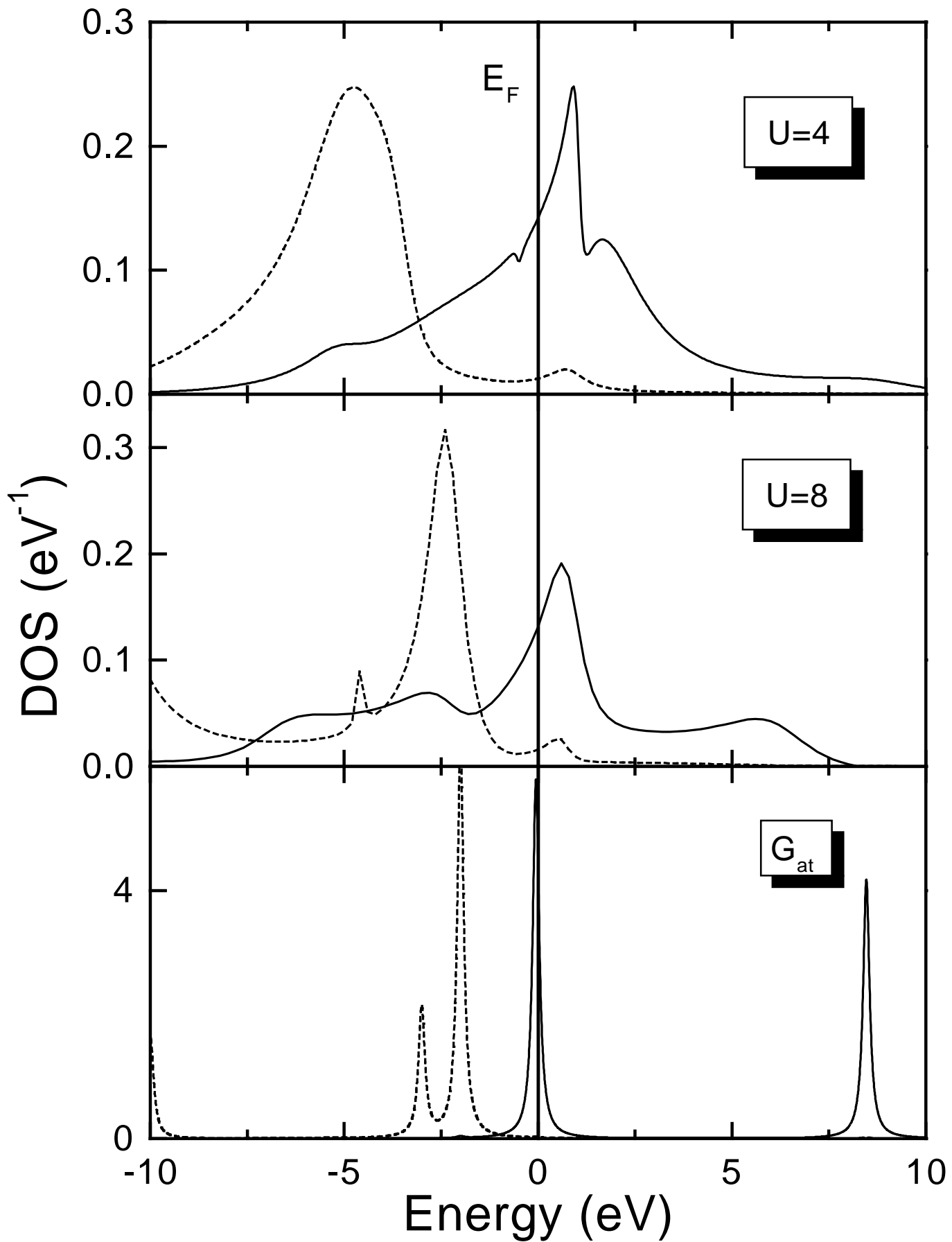
FIG. 9. Density of states for TmSe in HIA scheme in comparison with experimental XPS-spectrum [53] and results of paramagnetic LDA-calculations.





$A(\mathbf{k},\varepsilon)$ , arb. units





$A(\mathbf{k}, \varepsilon)$ , arb. units

